The Numerical Results of the Magnetic Behavior of the Thin-layers SFCL

Salah Belkhiri[1], F. Ben Mebarek[2], Mohamed. Lotfi. Khene[2]

[1] Department of Electrical Engineering, Faculty of technology, University of M'Sila, Algeria
[2] Department of Electrical Engineering, Faculty of technology, University of Biskra, Algeria
*corresponding author, E-mail: salah.belkhiri@univ-msila.dz

Abstract

The performance of superconducting current limiters associating the short-circuit phenomenon depends on the structure of the superconducting material envisaged and on the way of inserting it into the electrical network. The multi-layer structure, which uses thin "sandwich" layers, is found to be of interest in the search for fault current limiting power. In this paper, we present some numerical results of the magnetic behavior of superconducting fault current limiters (SFCLs). The numerical problem of this study is solved using the method of volume control (CVM). The electromagnetic and thermal coupling is ensured by an alternative algorithm. To describe the relationship between the electric field and the current density inside the thin-film superconductor, we chose to use the power law model widely used in simulation work.

1. Introduction

The object of the study is to design a thin-film superconducting current limiter capable of limiting short-circuit currents. Although thin-layers SFCL has certain favorable characteristics a priori (significant reduction in thermal stresses, relatively long service life, etc.). In this context, several simulation works have been proposed.

In this context, several simulation works have been proposed. In some of these works, the behavior of the superconductor is simulated as a vari-impedance [1-2], [3-4] where the superconducting material changes from non-dissipative state characterized by a zero impedance in the rated regime of the network to a very dissipative state characterized by a high impedance in the case of faults that can appear during the operation of the electrical network.

These simple models developed do not satisfactorily reflect the actual behavior of the superconductor in its intermediate state, particularly the flux-flow and flux-creep regimes [5,6,7]. For this, other microscopic models have been proposed in order to satisfactorily describe the flux-flow and flux-creep regimes [8-9]. In these models, the Maxwell equations are adopted and coupled to the heat diffusion equation, however the electromagnetic and thermal problems are solved in the case of one-dimensional [10] see bidimensional [11]. In these models, Maxwell's equations are adopted and coupled to the heat diffusion equation.

These models cannot correctly simulate superconducting current limiters, in particular, second generation superconducting current limiters.

The latter designed from several thin layers offer technical and economic advantages over conventional current limiter designed in a mass way is composed only of a superconducting material, usually type II. Thin-layers superconducting current limiters are essentially composed of three main layers (shunt, superconductor, substrate) [10], [9] and several buffer layers (Fig.2). Each layer has one or more functions defined [2]. They are produced by deposition on an assembly made up of a substrate and several buffer layers. The study of such a configuration requires the development of a three-dimensional computer code. For this, we propose in this article a three-dimensional mathematical-numerical model dedicated mainly to the modeling of thin-layers current limiters before and during the limitation process.

2. Formulation

To model the magnetic behavior of the presented problem, we adopted the formulation in magnetic vector potentials A and in electric scalar potential V, this one is described by the formulation below.

$$\nabla\times(\nu\nabla\times\mathrm{A})-\nabla(\nu\nabla\cdot\mathrm{A})+\sigma(E,T)\left(\frac{\partial\mathrm{A}}{\partial\mathrm{t}}+\nabla V\right)=\mathrm{J_s}$$
$$\nabla.\left\{-\sigma(E,T)\left(\frac{\partial\mathrm{A}}{\partial\mathrm{t}}+\nabla V\right)\right\}=0 \qquad (1)$$

$\boldsymbol{\upsilon}$ and $\boldsymbol{\sigma}$ represent respectively the magnetic reluctivity and the electrical conductivity of the superconductor. Concerning the apparent electrical conductivity of the superconducting material, in its non-dissipative state, it is defined by the ratio of J on E [12], this ratio is deduced from the characteristic E-J of the superconductor given by the relation.

$$\sigma_S(E,T) = \frac{J}{E} = \frac{J_c(T)}{E_c}\left(\frac{E}{E_c}\right)^{\frac{1}{n(T)}-1} \quad (2)$$

With $J_c(T) = J_{c0}\dfrac{(1-\frac{T}{T_c})}{(1-\frac{T_0}{T_c})}$

This relation reflects the superconductors flux-flow and Flux-Creep regimes that is to say if the superconductor is in a non-dissipative state, to complete the expression of the electrical conductivity of the superconductor in the dissipative regime. Add an additional term σ_n which translates the increase in the resistance of the superconductor. Thus, the apparent electrical conductivity of the superconductor is deduced by the relation.

$$\sigma(E,T) = \sigma_s(E,T) + \sigma_n(T) \quad (3)$$

Where J_C and E_C respectively represent the density of the critical current and the critical electric field. According to relation (3), the apparent conductivity of the superconductor depends on the electric field E and the temperature T reached within the material. The electric field E will be determined from the resolution of the electromagnetic problem described by the partial differential equation presented by the formulation (1). The temperature will be determined from the resolution of the heat diffusion problem presented by

$$\rho C_p(T)\frac{\partial T}{\partial t} - \nabla.\left(\kappa(T)\nabla T\right) = W \quad (4)$$

Where $\lambda(T)$, ρ, $Cp(T)$ are respectively the thermal conductivity in (W / K / m), the density in (Kg / m^3) and the specific heat of the material in (J / K / Kg), W is a power density in (W / m^3), it expresses all the losses generated in the superconducting current limiter expressed by

$$W = E.J \quad (5)$$

In the results of the simulations presented, the thermal and the electrical properties depend on the temperature as mentioned in the equations (1), (2), (3), (4). The Models describing this dependence are presented in [12].

The resolution of the system of equations 1 and 4 solves electromagnetic and thermal problems. These are defined by strongly nonlinear equations. To solve such a problem, several methods have been used mainly finite element method [8-9], it cannot ensure the convergence of the problem to be solved especially during the presence of a superconducting material where have used a power type law to define electrical conductivity (Equation 2). To avoid this type of problem we used the finite volume method in its three-dimensional version. The adopted mesh is of Cartesian or structured type, it consists of elementary volumes of hexahedral or cubic form. For each volume Dp of hexahedral shape, we associate a so-called main node P and six facets: e and w in the direction x, n and s in the direction y, t and b in the z direction (Fig.1). The neighboring volumes of Dp are represented by their close neighboring nodes: E and W along the x, N and S axis along the y, T and B axis along the z axis [12].

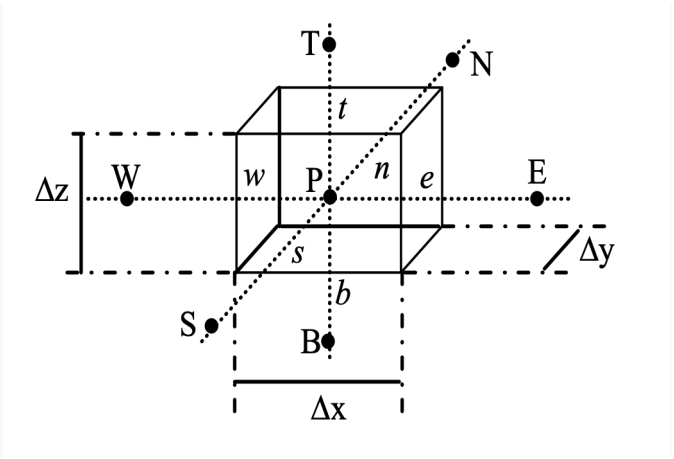

Figure 1: Elementary finished volume

$$\iiint_{D_P}\nabla\times(\upsilon\nabla\times\boldsymbol{A})\,d\tau - \iiint_{D_P}\nabla(\upsilon\nabla.\boldsymbol{A})d\tau + \iiint_{D_P}\sigma(\frac{\partial\boldsymbol{A}}{\partial t}+\nabla V)\,d\tau = \iiint_{D_P}\boldsymbol{J_s}\,d\tau$$

$$\iiint_{D_P}\nabla.\left\{-\sigma(\frac{\partial\boldsymbol{A}}{\partial t}+\nabla V)\right\}d\tau = 0 \quad (6)$$

$$\int_w^e\int_s^n\int_b^t \rho C_p\frac{\partial T}{\partial t}d\tau =$$

$$\int_w^e\int_s^n\int_b^t \frac{\partial}{\partial x}\left(\kappa\frac{\partial T}{\partial x}\right)d\tau + \int_w^e\int_s^n\int_b^t \frac{\partial}{\partial y}\left(\kappa\frac{\partial T}{\partial y}\right)d\tau + \int_w^e\int_s^n\int_b^t \frac{\partial}{\partial z}\left(\kappa\frac{\partial T}{\partial z}\right)d\tau + \int_w^e\int_s^n\int_b^t W d\tau \quad (7)$$

To calculate the derivative terms in (6) and (7), we consider in our study a linear variation of the magnetic potential and the temperature across the integration facets of the finite volume. After integration, we arrive at a system of algebraic equation below that will be solved by an algebraic method such as the Gausse-Seidel method that will be adopted in our problem. The integral of equations (6) and (7) leads to the following algebraic equations [12]:

$$cpA_x^P + \sigma_p D_p A_x^{\bullet P} = \left[\sum_{m=e,w...} c_m A_x^M + \sum_{\substack{i=y,z \\ m=e,w...}} q_m A_i^M + \frac{\sigma_p D_p}{\Delta x_e + \Delta x_w} \left(V^E - V^W \right) + J_{sx} D_p \right] \quad (8)$$

$$cpA_z^P + \sigma_p D_p A_z^{\bullet P} = \left[\sum_{m=e,w...} c_m A_z^M + \sum_{\substack{i=x,y \\ m=e,w...}} q_m A_i^M + \frac{\sigma_p D_p}{\Delta z_t + \Delta z_b} \left(V^T - V^B \right) + J_{sz} D_p \right] \quad (9)$$

$$V^P = \frac{1}{u_p} \left[\sum_{m=e,w...} u_m V^M + \sum_{\substack{i=x,y,z \\ m=e,n...}} cv_m A_i^{\bullet M} \right] \quad (10)$$

$$[C][\dot{T}] + [K][T] = [Q] \quad (11)$$

The electromagnetic and thermal coupling is ensured by the alternating coupling model.

3. Modeling of SFCL

The device constituting the studied limiter is of the conductor type deposited with YBaCuO, it consists of three main layers (shunt, superconductor and substrate) and several buffer layers. It is true that these are poor electrical and thermal conductors but they have a major and important role in the functioning of the SFCL. They also make it possible to create a chemical diffusion barrier preventing pollution of the superconductor by the elements of the substrate and preventing oxidation of the latter during the YBaCuO deposition phase. The simplified architecture adopted for a ribbon of length L rub is described in Figure.1.

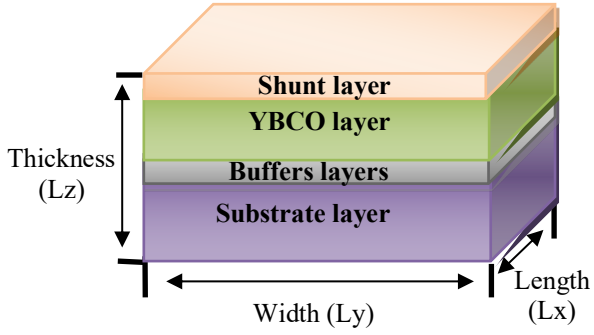

Figure 2: The description of the SFCL model.

Second-generation superconducting ribbons have been developed with the aim of getting as close as possible to the native properties of superconductors perfectly textured by epitaxial growth. The architecture of these ribbons is made in the form of a sandwich of four thin layers [15-16-17]: the substrate, the buffer layers, the superconducting layer and the shunt, (Fig. 1). Each layer has a role in the functioning of the limiter that we develop in the proposed model [14-16]. The substrate, which acts as a support, whose main function is to dissipate the excessive heat produced during the fault and thus protect the superconducting element. The thickness of the substrate is of the order of 100 µm [15-16-17], the alloys used are based on Nickel (NiCr, Inconel, Hastelloy, Constantan).

They make it possible to adapt the mechanical stresses, resulting on the one hand from the difference in thermal expansion coefficient between the superconductor and the substrate, on the other hand from the difference in the lattice parameter between these two materials. The buffer layers also provide a chemical diffusion barrier preventing pollution of the superconductor by the elements of the substrate and preventing oxidation of the latter during the YBaCuO deposition phase. They also make it possible to texturize the superconducting layer when the substrate has no orientation. To ensure a high critical current density for the YBaCuO, the buffer layer must provide a biaxial texture. The thickness of these layers varies between 0.5 µm and 3 µm [17], they are made up of YSZ, CeO, MgO or LZO. The superconducting layer generally of a thickness of the order of 1 µm (the YBaCuO) behaves like being a perfect conductor during the rated mode of the electrical network (R = 0) and in the blocked case limits the fault current by the insertion of a large resistance in the network [1]. The shunt has an average thickness of 200 nm, it acts as a thermal and electrical stabilizer in the blocked state of the limiter. Generally the materials used for this layer are noble materials such as gold or silver [16].

In the case without fault, only the YBCO is traversed by the current because its absence of resistance short-circuits the shunt, buffers and the substrate.

4. Simulation results

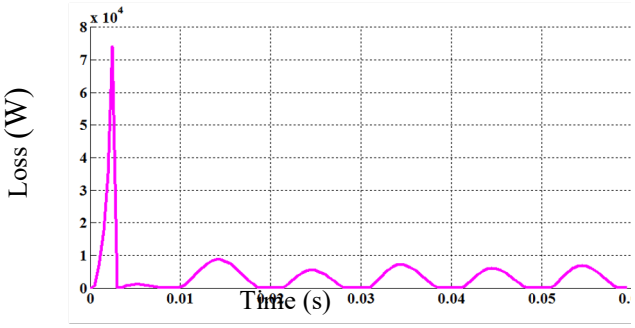

Figure 3: The variation of the average losses in the YBCO layer as a function of time.

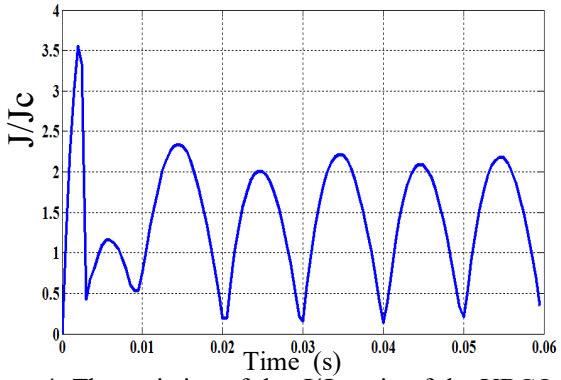

Figure 4: The variation of the ***J/Jc*** ratio of the YBCO layer as a function of time.

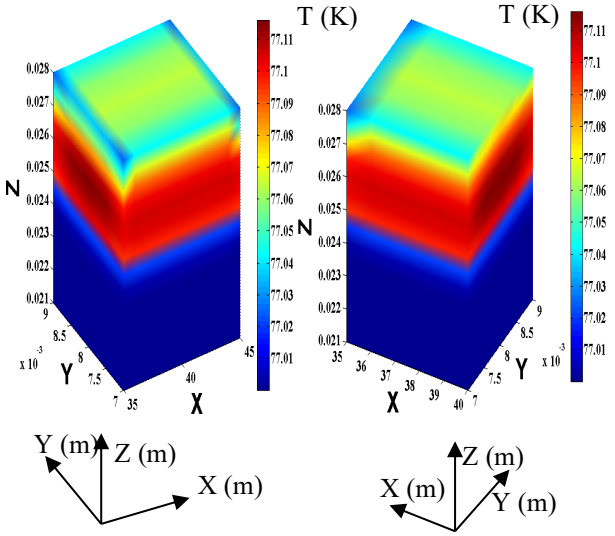

Figure 5: Spatial distribution of temperature within SFCL at t = 1 ms.

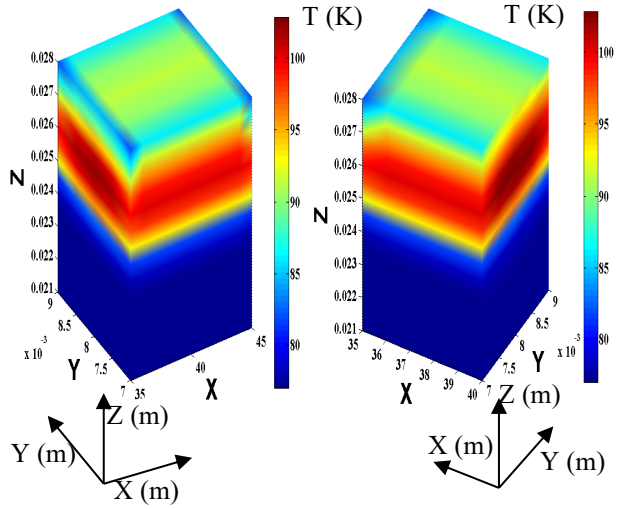

Figure 6: Spatial distribution of temperature within SFCL at t = 3 ms.

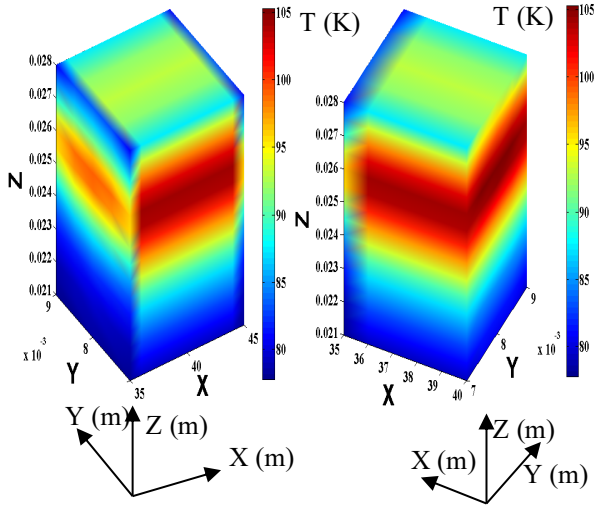

Figure 7: Spatial distribution of temperature within SFCL at t = 0.03s.

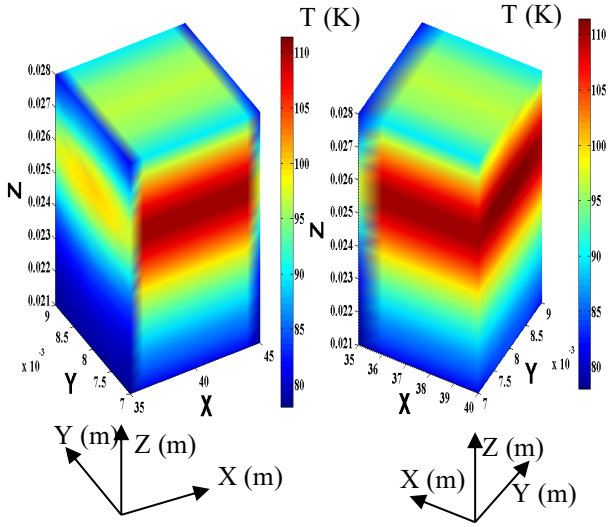

Figure 8: Spatial distribution of temperature within SFCL at t = 0.06s.

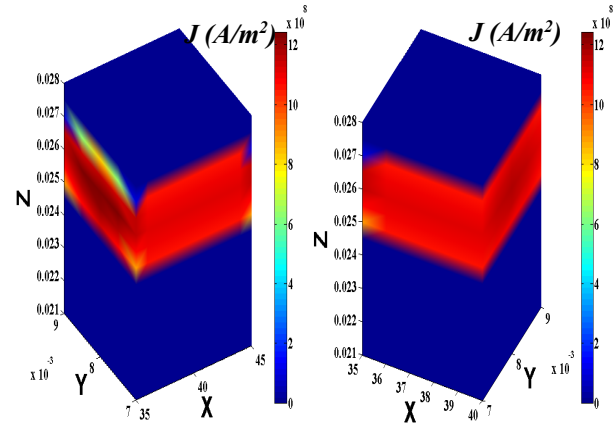

Figure 9: Spatial distribution of the density of current J within SFCL at t = 0.06s.

Figure (3) shows the temporal evolution of the average losses in the YBCO layer. The latter have evolved over time because of the energy dissipated per unit volume inside the superconducting zone (YBCO), there appears a strong increase in these losses at the start of the SFCL transition, and the amplitude reaches approximately 75KW. This is due to the heating caused by the increase in temperature within YBCO which is the site of considerably strong heat and which can damage the limiter. Then these losses are reduced, this is due to the substrate, whose main function is to dissipate the excessive heat produced during the short circuit fault and thus protect the superconducting layer.
According to the results presented in Fig. 5, we can say that the SFCL is always in a state supra at the instant t = 1 ms, that is to say that the current limiter cannot intervene at this time instant. The maximum temperature is almost 77.2 ° K below the critical temperature Tc = 92 ° K.

Figure 4 shows the variation of the J/Jc ratio as a function of time. It can clearly be seen that the superconducting limiter intervenes more quickly in a very short time even before the short - circuit current reaches its maximum during the first half-wave with a ratio of 3.5. The advantage of thin layers is their very rapid transitions, the current is limited for a J/Jc ratio generally less than or equal to two, through the substrate and the large specific surface area, the thin layers recover very quickly.

In Figs. 6-7, the temperature reached within the superconductor exceeds the value of the critical temperature (Tc = 92 ° K) at the instant t = 0.0025 s. Note also that this temperature is not homogeneous over the entire section of the limiter, in fact it is maximum at the center of the superconductor but it is minimal in the intermediate zones. The temperature which appears in the thin layers at the instant t> = 0.0025 s is mainly due to the transfer of heat between the superconducting layer and the thin layers. Indeed, during the time interval t <= 0.0025 s, all the current passes through the superconducting layer given its resistivity considered to be negligible compared to the resistivity's of the other layers. This means that the use of thin layers in the design of a current limiter has a great advantage as it significantly decreased the temperature within the current limiter during the process of fault current limiting. The decrease in temperature reached during the operation of the current limiter can extend the life of a superconducting current limiter. According to the results presented, we note that the use of thin layers has considerably improved the thermal behavior of the current limiter by significant reduction in temperature on the one hand, also the intermediate layers have improved the transition time or the current limiter intervenes in a shorter time. Also according to the results presented, it can be said that the presence of thin layers ensures that the temperature is maintained in the vicinity of 110 ° K (Fig. 8).

Fig. 9 shows the spatial distribution of current densities at SFCL breasts at time t = 0.06 s. It appears according to these results, that the current density reaches its maximum with a high concentration in the center of the YBCO layer, it is less in the other layers, and this is explained by the fact of its conductivities less low than that of YBCO even during the transition state.

5. Conclusions

The approach considered in this work takes into account the behavior of these layers according to their electromagnetic and thermal states. The different physical quantities and their spatial variations during the transition phase, current limitation and recovery are considered and widely exposed.

It is noted that when the short-circuit fault arises in the network, the current increases rapidly and exceeds the value of the critical current of the HTS which begins to transit. An electric field appears at its terminals and currents begin to flow through the shunt and the substrate.

The simulation results presented showed the interest and efficiency of thin films introduced in the design of a superconducting current limiter. These considerably improve the thermal stresses during the fault current limitation process by significantly reducing the temperature within the current limiter.

All these results will contribute to the optimization of the superconducting current limiter to obtain the best device for limiting the short-circuit currents and thus the best possible heat transfer. This is particularly important insofar as they can be used in the design of second generation limiters and installed in electrical networks.

References

[1] S.belkhiri, "Modeling a superconducting fault current limiter inserted in a nine-bus electrical network'', *AMSE. IIETA Journal*, Modelling. A, vol. 92, n°. 2-4, pp. 37-42, décembre 2019.

[2] S. Nemdili, S. Belkhiat, "Electrothermal Modeling of Coated Conductor for a Resistive Superconducting Fault-Current Limiter, " J Supercond Nov Magn doi10.1007/s10948-012-1895-4, 2012.

[3] J. Bae, Na and al, "Design and Tests of Prototype Hybrid Superconducting Fault Current Limiter WithFast Switch, " IEEE Trans. Appl. Supercond, vol. 22, no.3, pp. 5602604, 2012.

[4] H. Yamaguchi, and all. "Current Limiting Characteristics of Transformer Type Superconducting Fault Current Limiter With Shunt Impedance, " IEEE Trans. Appl. Supercond, vol.17, no. 2, pp. 1919-1922, 2007.

[5] S. Belkhiri, L. Alloui, F. B. Mebarek, "The influence of Geometrical Properties of Bulk Superconductors on Limiting Fault Current in an Electrical Network," ADVANCED ELECTROMAGNETICS, vol. 8, no.4, pp. 136-142, 2019.

[6] S. Belkhiri, M. Bouroubi, A. Harrabi, "Improvement of the Transient Stability of a 14-bus Network Using a

Superconducting Fault-Current Limiter SFCL," ADVANCED ELECTROMAGNETICS, vol. 9, no.2, pp. 75-83, 2020.

[7] S. Belkhiri, Z. Ghemari, "Comparative Study of Solid and Thin-Layers Superconducting Fault Current Limiters SFCL for Electrical Network Transient Stability Improvement," Journal of Superconductivity and Novel Magnetism. Vol. 35, Nº 3, pp.679-688, 2022. https://doi.org/10.1007/s10948-021-06128-x

[8] W. K. Chan, and al. "Three-Dimensional Micrometer-Scale Modeling of Quenching in High-Aspect-RatioYBa2Cu3O7−δ Coated Conductor Tapes—Part I: Model Development and Validation, " IEEE Trans. Appl. Supercond., vol. 20, no. 6, pp. 2370–2379, 2010.

[9] W. K. Chan, and al. "Three-Dimensional Micrometer-Scale Modeling of Quenching in High-Aspect-RatioYBa2Cu3O7−δ Coated Conductor Tapes—Part II: Influence of Geometric and Material Properties and Implications for Conductor Engineering and Magnet Design, "IEEE Trans. Appl. Supercond, vol. 21, no. 6, pp. 2628–2634, 2011.

[10] K. Nam, and al. "Thermal and Electrical Analysis of Coated Conductor Under AC Over-Current, " IEEE Trans. Appl. Supercond, vol. 17, no. 2, 1923-1926, 2007.

[11] Casali and al. "Two-Dimensional Anisotropic Model of YBCO Coated Conductors, " IEEE Trans. Appl. Supercond, vol. 25, no. 1, pp. 6600112, 2015.

[12] L. Alloui, F. Bouillault, and S.M. Mimoune, "Numerical Study of the Influence of flux creep and of Thermal Effect on Dynamic Behaviour of Magnetic Levitation Systems with a high-Tc superconductor using control volume method, " EPJ. App. Phys, vol. 37, no. 2, pp. 191-195, 2009.

[13] Y. Yoshida, M. Uesaka, and K. Miya, "Magnetic field and force analysis of high Tc superconductor with flux flow and creep, " IEEE Trans. Magn, vol.30, no. 5, pp. 3503-3506, 1994.

[14] C. Gandioli, P. Tixador, G. Mariani. "Tests and simulations of different YBCO tapes for FCL, " IEEE Transactions on Applied Superconductivity, vol. 22, no. 3, pp. 5603104–5603104, 2012.

[15] Y. Cointe, Doctorat Thesis, "Continuous superconductive limiter," Engineering Sciences [physics]. National Polytechnic Institute of Grenoble - INPG, 2007. French. <Tel-00300552>.

[16] L. Cavallucci, Doctorat Thesis, "Thermal stability and AC losses in high-field Superconducting magnets," Biomedical Electrical Engineering and IBES Systems Cycle XXX, 2018.

[17] W.T.B.d.Souse, Doctorat Thesis, " Transient simulations of superconducting fault current limiters," Electrical Engineering, Federal University of Rio de January, 2015.